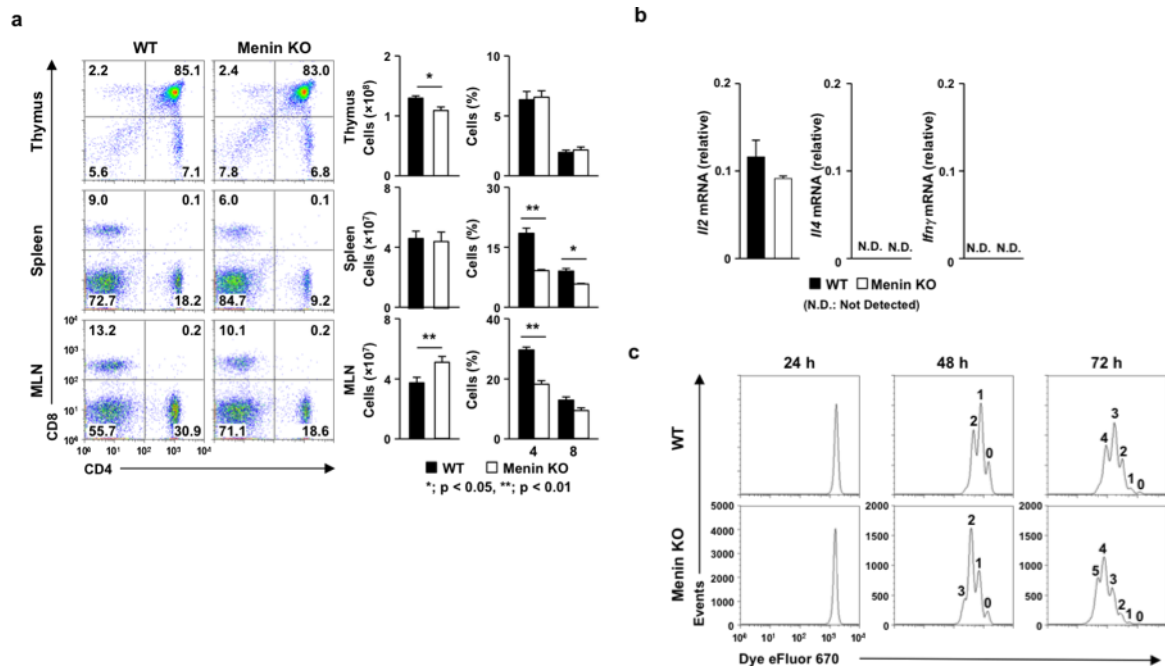
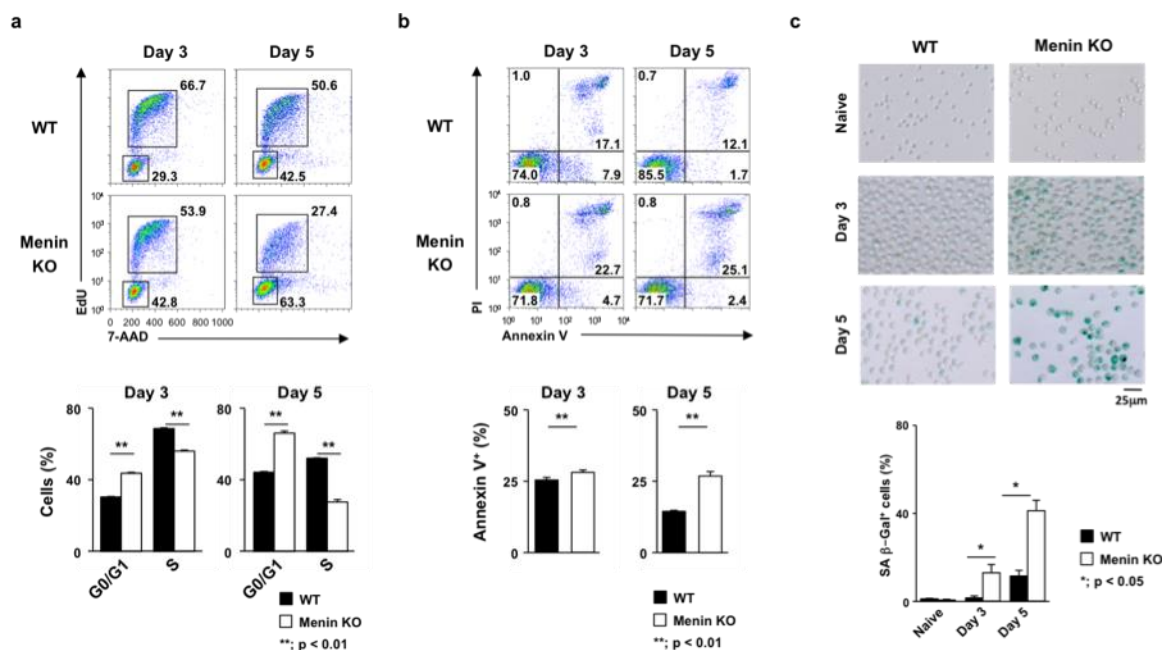


**Supplementary Information****The Menin–Bach2 axis is critical for regulating CD4 T cell senescence and cytokine homeostasis**

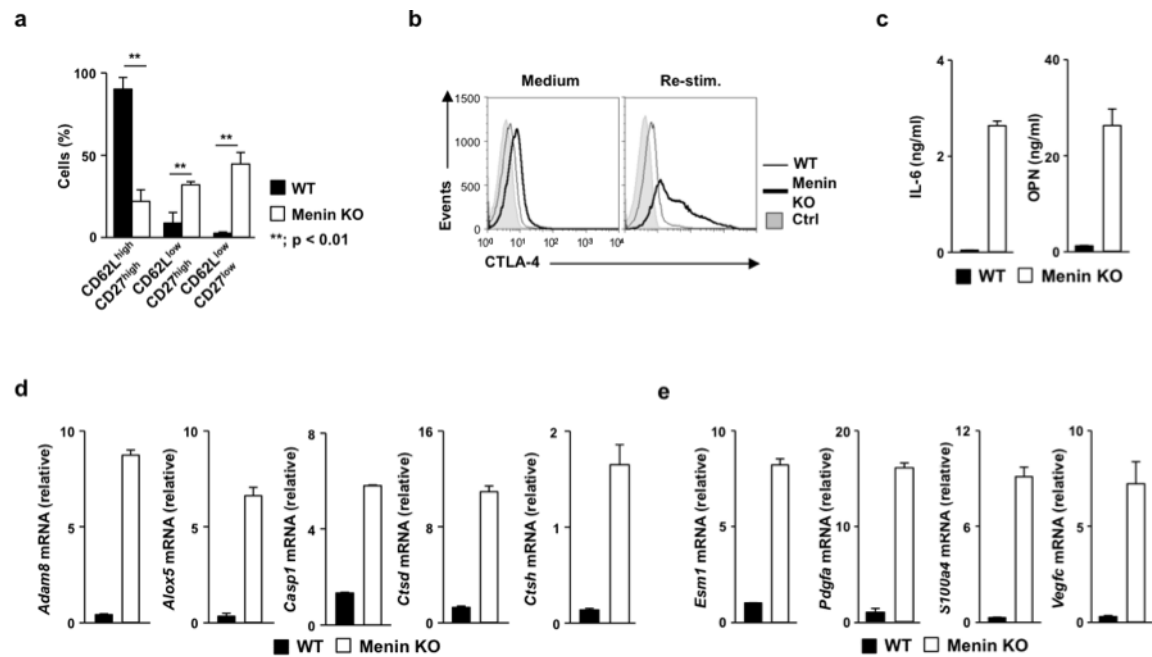
Makoto Kuwahara, Junpei Suzuki, Soichi Tofukuji, Takeshi Yamada, Makoto Kanoh,  
Akira Matsumoto, Saho Maruyama, Kohei Kometani, Tomohiro Kurosaki, Osamu  
Ohara, Toshinori Nakayama & Masakatsu Yamashita



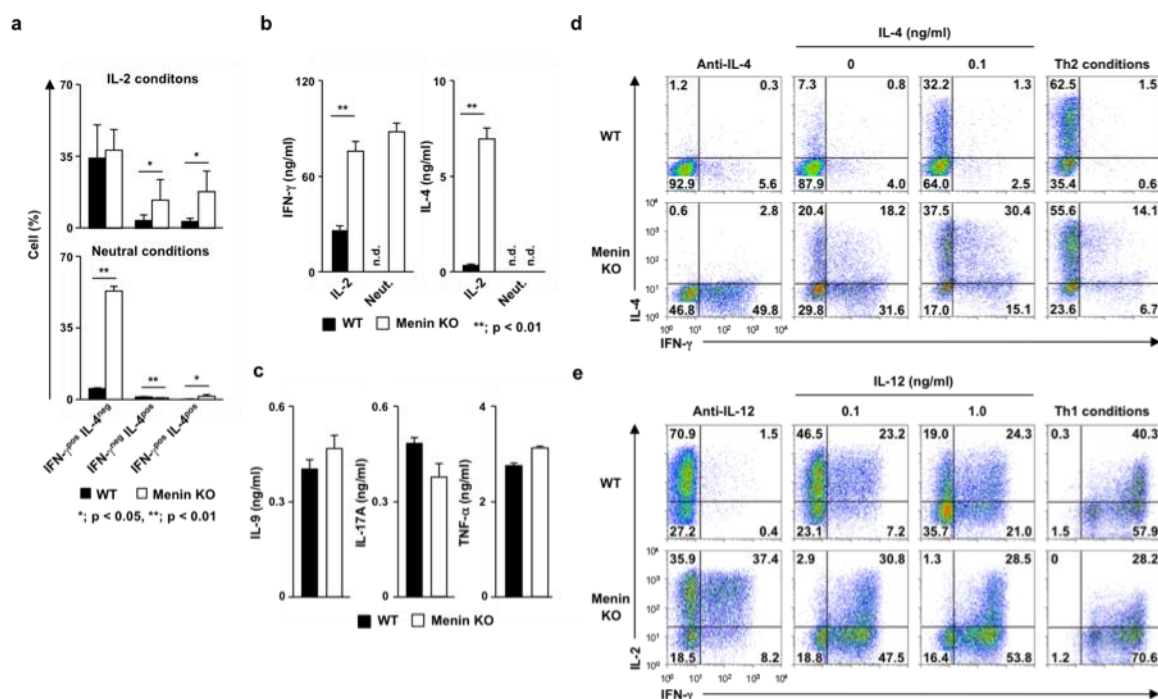
**Supplementary Figure 1. Phenotypic characterization of the Menin KO CD4 T cells.** (a) Representative CD4/CD8 profiles of the thymocytes, splenocytes, mesenteric lymph node cells of Menin KO (*Menin*<sup>fl/fl</sup> × CD4-Cre TG) mice. Cell numbers of indicated organs from the Menin KO mice are shown with standard deviations (n = 5; right panel). (b) The results of the quantitative reverse transcriptase polymerase chain reaction (RT-PCR) analysis of cytokine mRNA expression in the WT and Menin KO naïve CD4 T cells stimulated with a combination of immobilized anti-TCR-β mAb and soluble anti-CD28 mAb for 2 h. (c) Proliferative responses of the Menin KO naïve CD4 T cells. Naïve CD4 T cells from WT and Menin KO mice were labeled with Dye eFluor<sup>®</sup> 670 and stimulated with a combination of immobilized anti-TCR-β mAb and soluble anti-CD28 mAb.



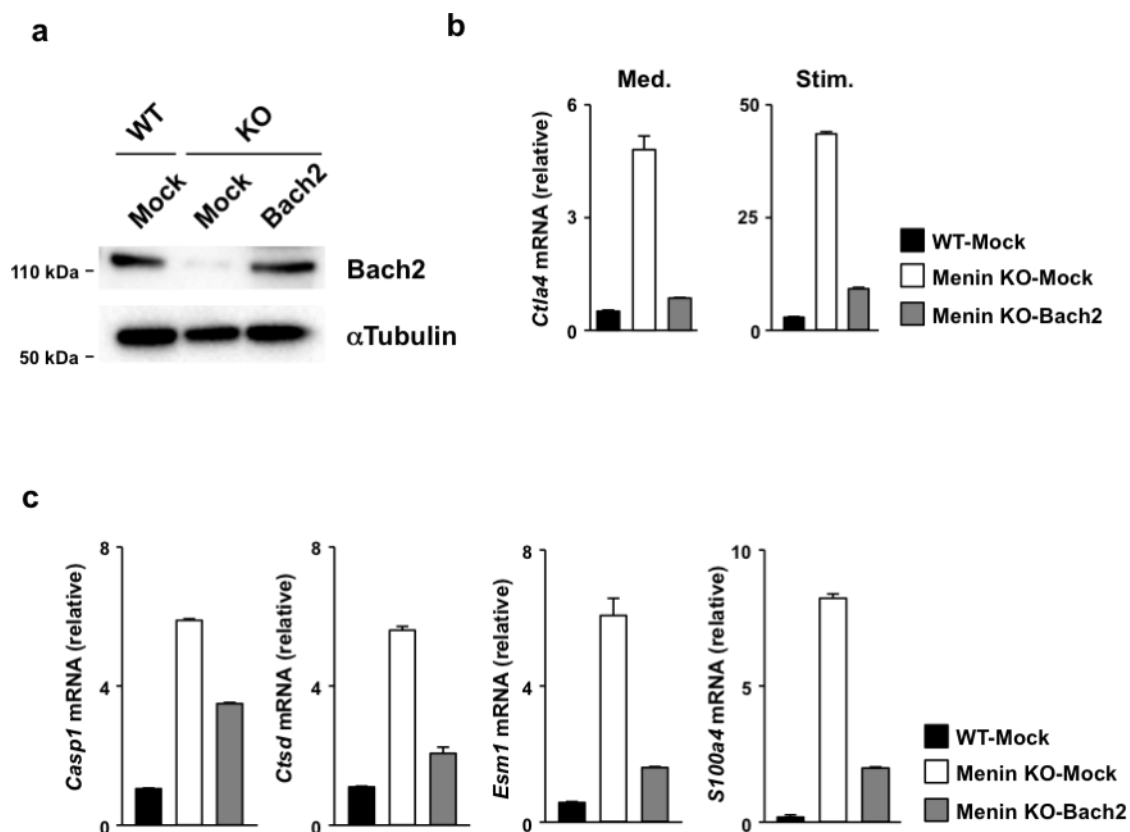
**Supplementary Figure 2. The effects of Menin deficiency on the cell cycle, cell death and SA  $\beta$ -Gal activity in activated CD4 T cells.** (a) The results of the cell cycle analysis of CD4 T cells from the Menin KO and WT mice cultured under IL-2-conditions for 3 or 5 days, respectively. The percentages of G0/G1 and S phase cells in three independent cultures with the standard deviations are shown (lower). (b) The results of the cell death analysis of CD4 T cells from the WT and Menin KO mice on day 3 and 5, respectively. The percentages of annexin V positive cells in three independent cultures with the standard deviations are shown (lower). (c) SA  $\beta$ -galactosidase (SA  $\beta$ -Gal) staining of the Menin KO and WT control naïve CD4 T cells,  $T_H$  cells cultured under IL-2-conditions for 3 and 5 days, respectively. The percentages of SA  $\beta$ -Gal-positive cells in three independent cultures with the standard deviations are shown (lower).



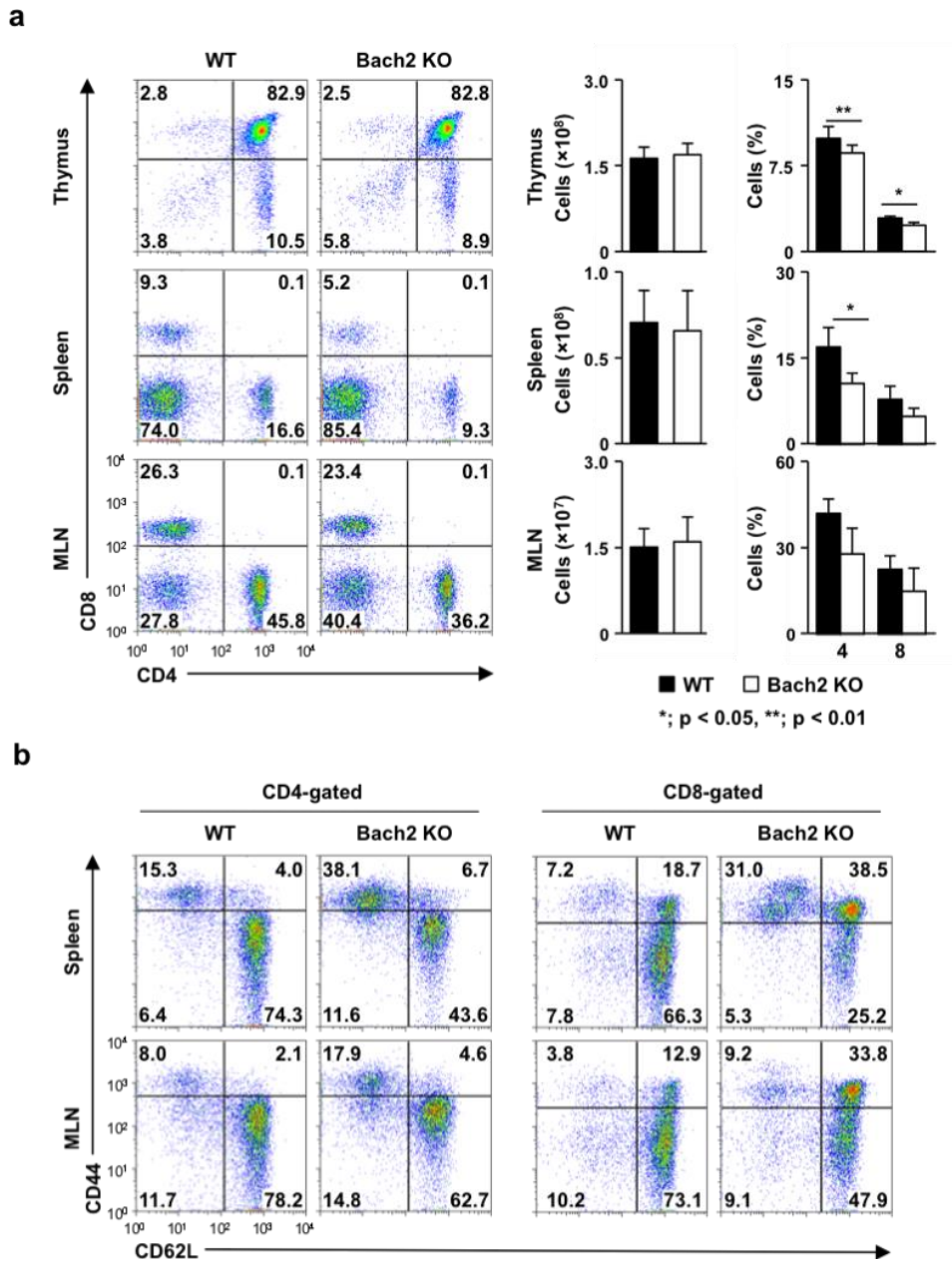
**Supplementary Figure 3. Phenotypic characterization of the Menin KO effector CD4 T cells.** (a) The percentages of CD62L<sup>high</sup>/CD27<sup>high</sup>, CD62L<sup>low</sup>/CD27<sup>high</sup> and CD62L<sup>low</sup>/CD27<sup>low</sup> cells in three independent cultures with the standard deviations are shown (right). (b) The cell-surface expression of CTLA-4 on the WT or Menin KO T<sub>H</sub> cells with (right) or without (left) TCR restimulation (4 h). (c) The ELISA IL-6, and OPN in supernatants of naïve CD4 T cells cultured under IL-2 conditions for 5 days and restimulated with an immobilized anti-TCR-β for 16 h. (d and e) The results of the quantitative RT-PCR analysis of mRNA encoding pro-inflammatory enzymes and pro-angiogenic factors (vertical axes) in the naïve CD4 T cells cultured under IL-2 conditions for 5 days.



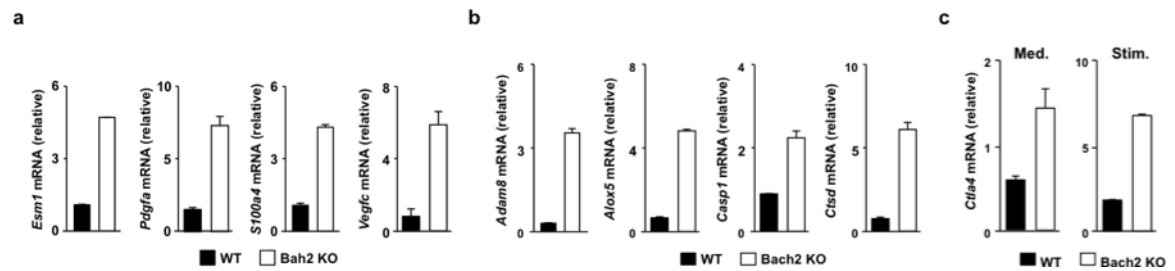
**Supplementary Figure 4. The enhanced generation of IFN- $\gamma$ - and IL-4-producing cells in the Menin KO CD4 T cell cultures.** (a) The percentages of IFN- $\gamma$ -, IL-4- and IFN- $\gamma$ /IL-4 double producing cells in three independent cultures are shown. (b) The ELISA of cytokines (IFN- $\gamma$  and IL-4) in supernatants of the naïve CD4 T cells cultured under IL-2 conditions or neutral conditions for five days and restimulated with an immobilized anti-TCR- $\beta$  for 16 h. (c) The ELISA of cytokines (IL-9, IL-17A, and TNF- $\alpha$ ) in supernatants of the naïve CD4 T cells cultured under IL-2 conditions for 5 days and restimulated with an immobilized anti-TCR- $\beta$  for 16 h. (d) The results of the intracellular FACS analysis of IL-4 and IFN- $\gamma$  in the WT and Menin KO naïve CD4 T cells stimulated with immobilized anti-TCR- $\beta$  and soluble anti-CD28 mAb in the presence of endogenously produced IL-4, exogenously added IL-4 (0.1 ng/ml), anti-IL-4 mAb or T<sub>H</sub>2 conditions for 5 days are shown. (e) The intracellular staining of IFN- $\gamma$  and IL-2 in the WT and Menin KO naïve CD4 T cells stimulated with immobilized anti-TCR- $\beta$  and soluble anti-CD28 mAb in the presence of various concentrations of IL-12 in the presence of an anti-IFN- $\gamma$  mAb and anti-IL-4 mAb or T<sub>H</sub>1-polarizing conditions for 5 days are shown.



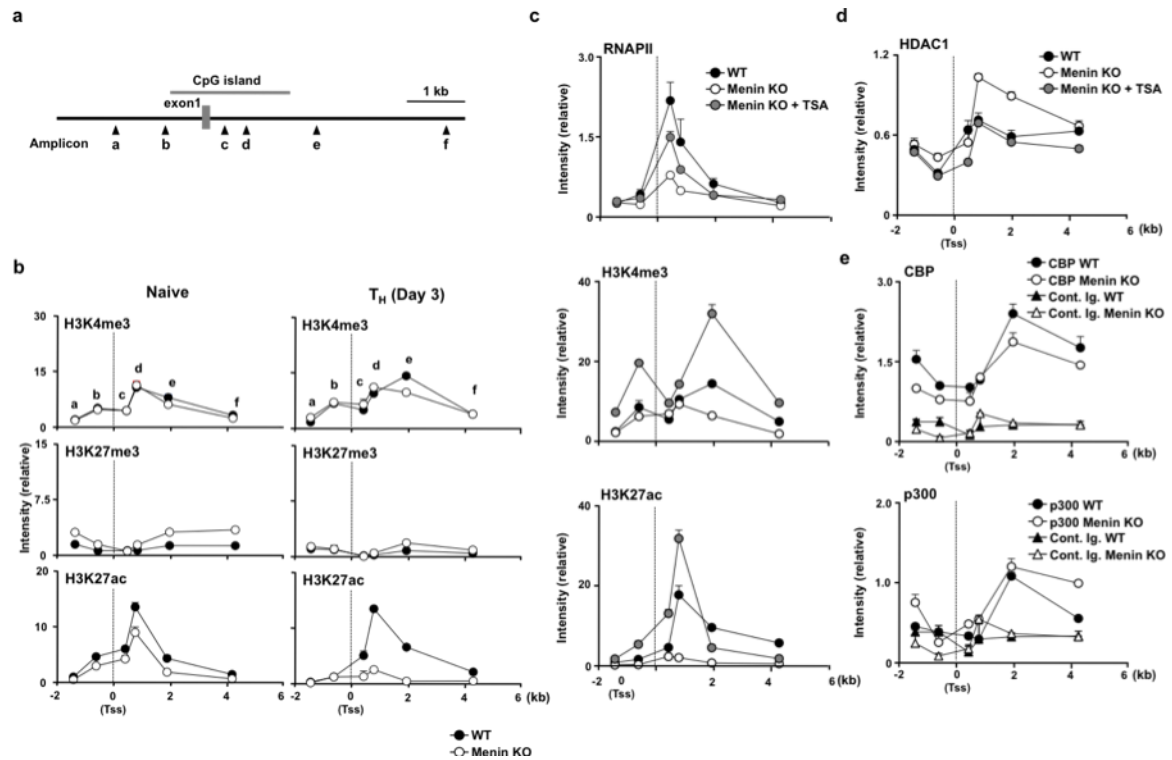
**Supplementary Figure 5. The mRNA expression profiles in the *Bach2*-transduced Menin KO T<sub>H</sub> cells.** (a) The results of the immunoblot analysis of Bach2 in the nuclear fractions of the *Bach2*-transduced Menin KO T<sub>H</sub> cells. Mock- or *Bach2*-transduced T<sub>H</sub> cells were purified using an AutoMACS device. (b) The results of the quantitative RT-PCR analysis of *Ctla4* with or without immobilized anti-TCR- $\beta$  restimulation for four hours. The results are presented relative to the mRNA expression of *Hprt*. (c) The results of the quantitative reverse transcriptase polymerase chain reaction (RT-PCR) analysis of mRNAs encoding pro-inflammatory enzymes and pro-angiogenic factors (vertical axes) in the *Bach2*-transduced Menin T<sub>H</sub> cells.



**Supplementary Figure 6. The T cell development in the *Bach2*<sup>fl/fl</sup> × CD4-Cre TG mice.** (a) Representative CD4/CD8 profiles of the thymocytes, splenocytes and mesenteric lymph node cells from the Bach2 KO (*Bach2*<sup>fl/fl</sup> × CD4-Cre TG) mice. Cell numbers of indicated organs from the Bach2 KO mice are shown with standard deviations (n = 5; right panel). (b) Representative CD62L/CD44 profiles of the CD4 or CD8 T cells from the spleen of the WT and Bach2 KO mice.

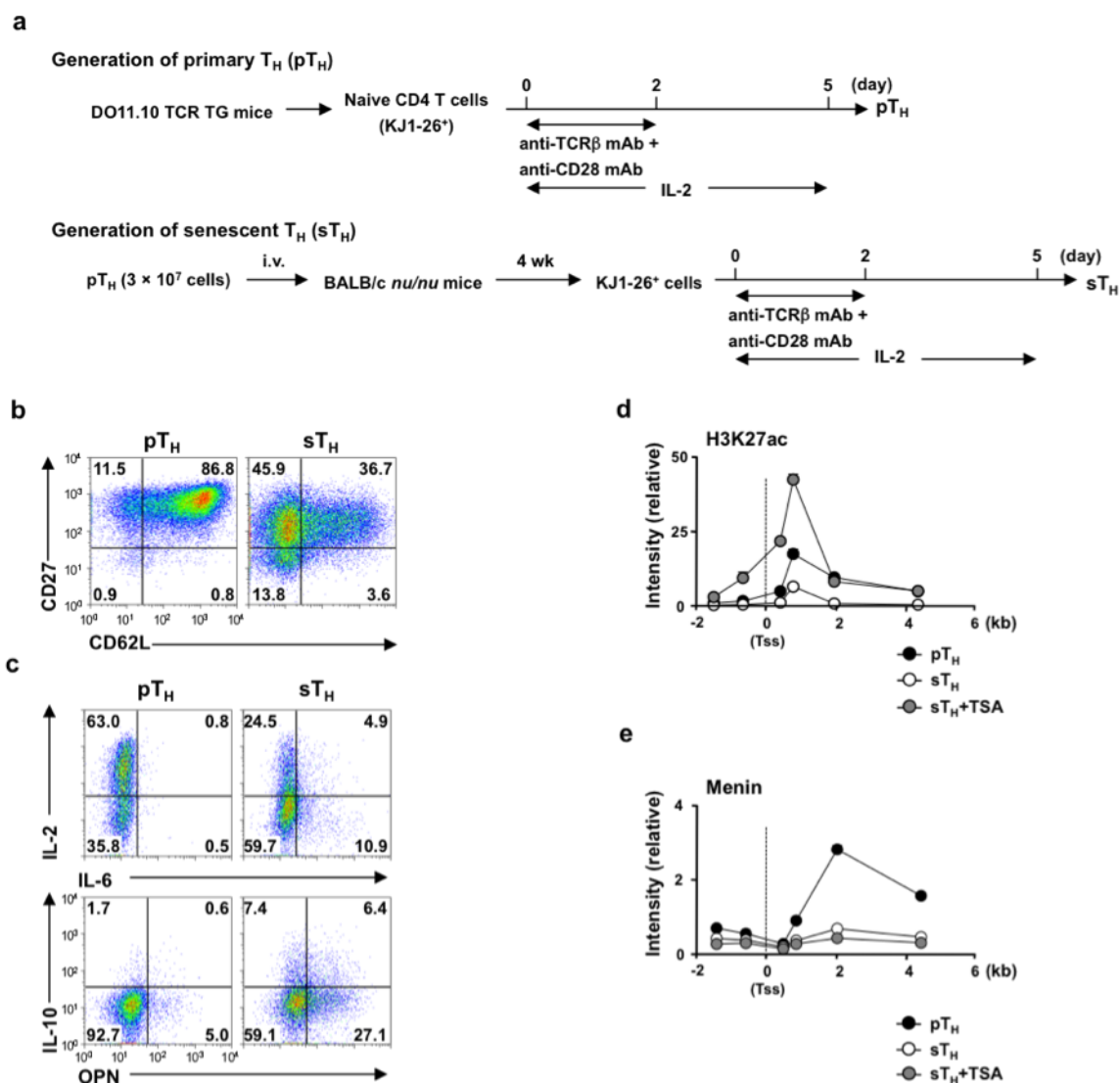


**Supplementary Figure 7. The mRNA expression profiles in the Bach2 KO T<sub>H</sub> cells.** (a) The results of the quantitative RT-PCR analysis of mRNA encoding pro-inflammatory enzymes (vertical axes) in the Bach2 KO T<sub>H</sub> cells. The results are presented relative to the mRNA expression of *Hprt*. (b) The results of the quantitative RT-PCR analysis of mRNA encoding pro-angiogenic factors (vertical axes) in the Bach2 KO T<sub>H</sub> cells. (c) The results of the quantitative RT-PCR analysis of *Ctla4* mRNA in the Bach2 KO T<sub>H</sub> cells with (right) or without (left) the TCR restimulation. All experiments were performed with T<sub>H</sub> cells cultured under IL-2 conditions for 7 days.



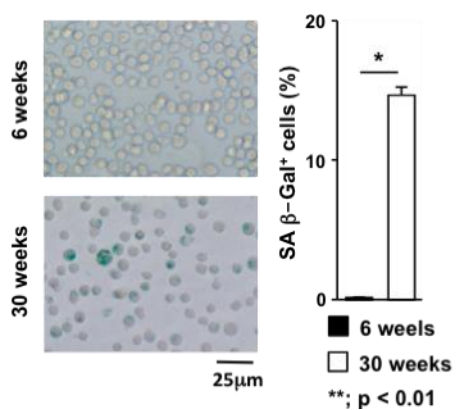
**Supplementary Figure 8. The epigenetic analysis at the *Bach2* gene locus in the Menin KO  $T_H$  cells.** (a) A schematic representation of the region surrounding the Tss of the *Bach2* locus. The locations of the PCR primer pairs (Amplicon) used in the manual ChIP assay are also listed. (b) The results of the ChIP with a quantitative PCR analysis of the histone modification (H3K4me3, H3K27ac, and H3K27me3) status around the Tss of the *Bach2* in the WT and Menin KO naïve CD4 T cells, and  $T_H$  cells cultured under IL-2 conditions for 3 days. The relative intensity (/input) with the standard deviation is shown. (c) The results of the ChIP with a quantitative PCR analysis of the RNA polymerase II binding, and histone modification status (H3K4me3 and H3K27ac) around the Tss of the *Bach2* in the TSA-treated Menin KO  $T_H$  cells. The relative intensity (/input) with the standard deviation is shown. (d) The results of the ChIP with a quantitative PCR analysis of the HDAC1 around the Tss of the *Bach2* in the TSA-treated Menin KO  $T_H$  cells. The relative intensity (/input) with the standard deviation is shown. (e) The results of the ChIP with quantitative PCR analysis of CBP (left) and p300 (right) binding around the Tss of *Bach2* in the WT and Menin KO  $T_H$  cells. The relative intensity (/input) with the standard deviation is shown. The

experiments (**c**, **d** and **e**) were performed with T<sub>H</sub> cells cultured under IL-2 conditions for 5 days.



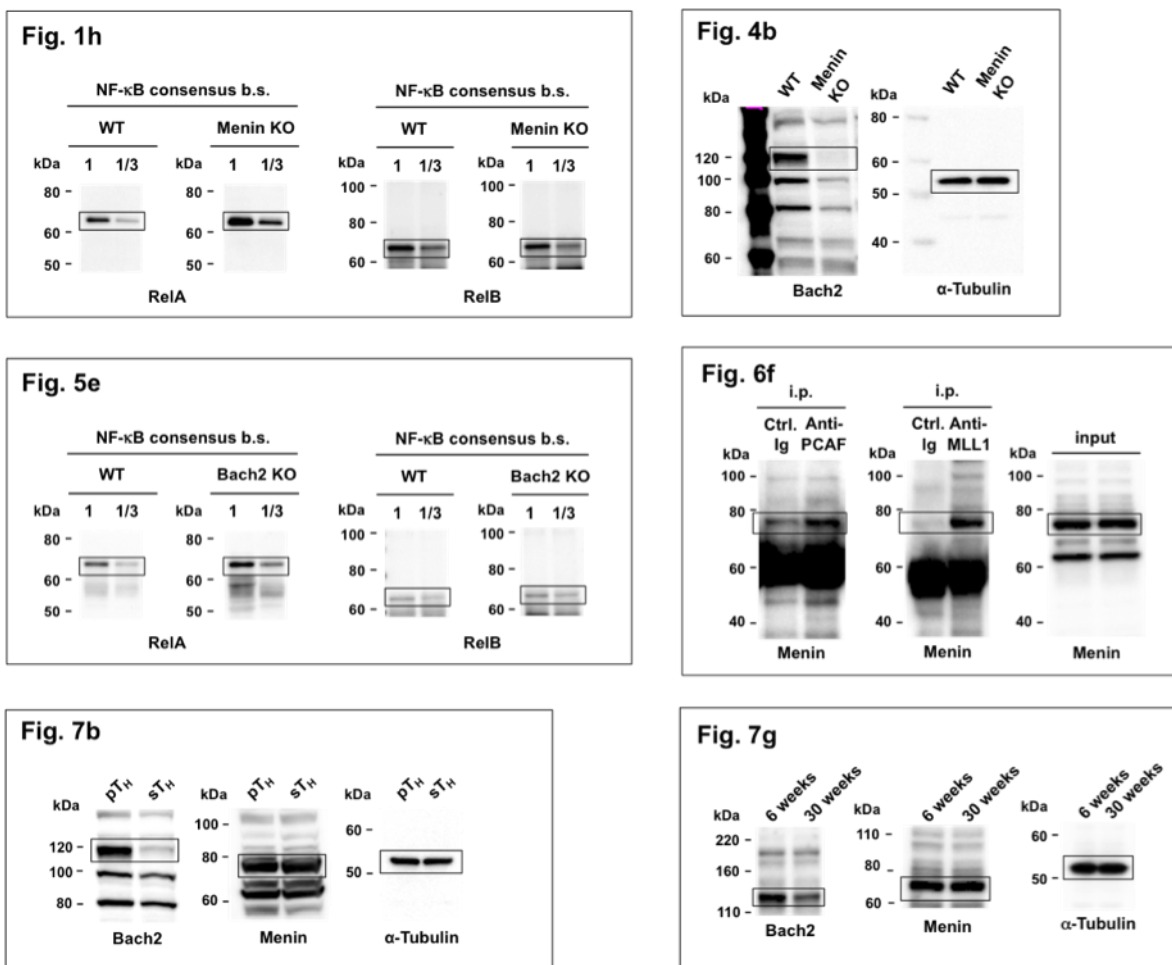
**Supplementary Figure 9. The generation and phenotypic characterization of senescent CD4 T cells.** (a) A scheme of the protocol for the generation of senescent CD4 T cells. In brief, KJ1<sup>+</sup> naïve CD4 T cells from DO11.10 OVA-specific TCR TG mice were stimulated with plate bound anti-TCR-β mAb plus anti-CD28 mAb in the presence of IL-2 for 2 days, and then cells were further expanded with IL-2 another 3 days *in vitro*. We termed these cells “primary effector CD4 T (pT<sub>H</sub>) cells”. The pT<sub>H</sub> were transferred intravenously into syngeneic BALB/c nu/nu recipient mice to induce homeostatic expansion *in vivo*. Four weeks after transfer, KJ1<sup>+</sup> transferred CD4 T cells were recovered from the spleen of recipient mice, and expanded same way as primary stimulation. The secondary expanded effector CD4 T cells, we termed “senescent effector CD4 T (sT<sub>H</sub>) cells”. (b) The staining profile of CD62L/CD27 on

the cell surface of the pT<sub>H</sub> and sT<sub>H</sub>. The cell numbers are indicated in each quadrant. (c) The results of the intracellular FACS analysis of IL-2/IL-6 and IL-10/OPN in the pT<sub>H</sub> or sT<sub>H</sub> cells stimulated with plate bound anti-TCR- $\beta$  mAb for 6 h. The cell numbers are indicated in each quadrant. (d) The results of the ChIP with a quantitative PCR analysis of the H3K27ac status around the Tss of the *Bach2* in the TSA-treated sT<sub>H</sub> cells. The relative intensity (/input) with the standard deviation is shown. (e) ChIP with quantitative PCR analysis for the binding of Menin to the *Bach2* Tss region in TSA-treated sT<sub>H</sub> cells. The relative intensity (/input) with the standard deviation is shown.



**Supplementary Figure 10. Increased SA  $\beta$ -Gal activity in the elderly T<sub>H</sub> cells.**

SA  $\beta$ -galactosidase (SA  $\beta$ -Gal) staining of the young (6 weeks old) and elderly (30 weeks old) T<sub>H</sub> cells (left). The percentages of SA  $\beta$ -Gal-positive cells in three independent cultures with the standard deviations are shown (right).



**Supplementary Figure 11. Representative entire images of immunoblotting and SDS-PAGE. Boxed areas were cropped for designated figures.**

## Supplementary Methods.

### Primers and probes

Specific primers, and Roche Universal Probes used in quantitative reverse transcriptase polymerase chain reaction were as follows: *Hprt*: 5' TCCTCCTCAGACCGCTTT 3' (forward), 5' CCTGTTTCATCATCGTAATC 3' (reverse), probe #95; *Menin*: 5' ACCCACTCACCCCTTTATCACA 3' (forward), 5' ACATTTTCGGTTGCGACAT 3' (reverse), probe #20; *Bach2*: 5' CAGTGAGTCGTGTCCTGTGC 3' (forward), 5' TTCCTGGGAAGGTCTGTGAT 3' (reverse), probe #79; *Gzma*: 5' GGCCATCTCTTGCTACTCTCC 3' (forward), 5' CGTGTCTCCTCCAATGATTCT 3' (reverse), probe #75; *Gzmb*: 5' GCTGCTCACTGTGAAGGAAGT 3' (forward), 5' TGGGGAATGCATTTTACCAT 3' (reverse), probe #2; *Gzmc*: 5' TGGGAGACTCAAAGATCAAGG 3' (forward), 5' TGCAGCTGCTCTTTTACACAC 3' (reverse), probe #101; *Gzmd*: 5' TGACCCTACTTCTGCCTCTCAG 3' (forward), 5' GGGAGTGTGGCTTCACCA 3' (reverse), probe #82; *Gzme*: 5' CCCTACTTCTGCCTCTTGGGA 3' (forward), 5' ATGTAGGGGAGGGAGTGT 3' (reverse), probe #82; *Gzmf*: 5' GACCCTTCTTCTGCCTCTCAG 3' (forward), 5' GAGTGGGGCTTGACCTCAT 3' (reverse), probe #82; *Gzmg*: 5' CTGGGAAGATGCCACCAA 3' (forward), 5' GGAGTGTGGCTTCACCTCAT 3' (reverse), probe #2; *Prf1*: 5' AATATCAATAACGACTGGCGTGT 3' (forward), 5' ATGTAGGGGAGGGAGTGT 3' (reverse), probe #42; ; *Pmaip1*: 5' CAGATGCCTGGGAAGTCG 3' (forward), 5' TGAGCACACTCGTCCTTCAA 3' (reverse), probe #15; *S100a4*: 5' GGAGCTGCCTAGCTTCCTG 3' (forward), 5'

TCCTGGAAGTCAACTTCATTGTC 3' (reverse), probe #56; *Esm1*: 5'  
 CAGTATGCAGCAGCCAAATC 3' (forward), 5' GATGCTGAGTCACGCTCTGT 3'  
 (reverse), probe #16; *Ctla4*: 5' TCACTGCTGTTTCTTTGAGCA 3' (forward), 5'  
 GGCTGAAATTGCTTTTCACAT 3' (reverse), probe #21; *Cdkn1a*:  
 5'-TCCACAGCGATATCCAGACA-3' (forward), 5' GGACATCACCAGGATTGGAC  
 3' (reverse), probe #21; *Perp*: 5' GACCCCAGATGCTTGTTC 3' (forward), 5'  
 ACCAGGGAGATGATCTGGAA 3' (reverse), probe #71; *p19<sup>Arf</sup>*: 5'  
 GGGTTTTCTTGGTGAAGTTCG 3' (forward), 5' TTGCCATCATCATCACCT 3'  
 (reverse), probe #106; *Cdkn2a*: 5' AATCTCCGCGAGGAAAGC 3' (forward), 5'  
 GTCTGCAGCGGACTCCAT 3' (reverse), probe #91; *Cdkn2b*: 5'  
 GGCTGGATGTGTGTGACG 3' (forward), 5' GCAGATACCTCGCAATGTCA 3'  
 (reverse), probe #41; *Vegfc*: 5' CAGACAAGTTCATTCAATTATTAGACG 3' (forward),  
 5' CATGTCTTGTAGCTGCCTGA 3' (reverse), probe #53; *Pdgfra*: 5'  
 GTGCGACCTCCAACCTGA 3' (forward), 5' GGCTCATCTCACCTCACATCT 3'  
 (reverse), probe #52

The specific primers and Roche Universal probes used in ChIP-qPCR were as follows:

a: 5' GAATCGGGTACCCAGGAAAG 3' (forward), 5'  
 GGTGACAGTGCCTACGCTAGT 3' (reverse), probe #56; b: 5'  
 GGCTTTCCCTTTGATGAAGTG 3' (forward), 5' CTAGTGGGGTTGGGAGAGC 3'  
 (reverse), probe #21; c: 5' CCGGGTGTTCGGAACAG 3' (forward), 5'  
 CGCCCCACGACTGACTTA 3' (reverse), probe #52; d: 5'  
 CCAAGAGGGGACACCTTGTA 3' (forward), 5' GCACACAGGTGTGGATGTGT 3'

(reverse), probe #7; e: 5' GCGCTTATAATCACCACAAAAC 3' (forward), 5'

GCCAAAGTGGGTGATCAATAG 3' (reverse), probe #2; f: 5'

GCAAGTTGCGATTTGAACC 3' (forward), 5' CACAAGCAGCAGGCTGAA 3'

(reverse), probe #68